

# Bifurcation analysis of the metabolism of *E. coli* at optimal enzyme levels

Francisco G. Vital-Lopez, Costas D. Maranas, and Antonios Armaou\*, *Member, IEEE*

**Abstract** — Understanding the metabolic function of microorganisms has recently received a lot of attention due to its importance in fields such as health and industry. Metabolism in microorganisms is a sophisticated process comprised of several thousands of different components with intricate interactions between them. This characteristic is translated into complex dynamical behavior that such systems can exhibit e.g., multiple steady states, hysteresis, or oscillations. Kinetic models of the processes occurring in the cells allow us not just to determine optimal conditions for a given objective but also to assess their stability properties. In this work we evaluate the stability of the central carbon metabolism of *E. coli*, using the Chassagnole *et al.* model, at optimal enzyme levels as determined by [1] for the production of serine. To accomplish this, we construct bifurcation diagrams considering the level of one, two and three enzymes as bifurcation parameters. We determine that the system goes through a Hopf bifurcation and/or a limit point for certain parameter values. This is achieved for a 68% change in the enzyme level, implying that the system is robust to perturbations on the process parameters at the optimal enzyme levels for the employed model description.

## I. INTRODUCTION

METABOLISM is a process that involves a large number of enzymes and sophisticated regulation mechanisms, through which the cell converts thousand of organic compounds into the biomolecules and energy needed to support their life. The main approaches on the analysis of metabolism are based either on stoichiometry or the kinetics of the enzymatic reactions that take place in the cell. The first methodologies characterize the space, constrained by the stoichiometry, of the possible flux distributions [2-6]. These approaches allow us to evaluate possible flux distributions and the effect of changes in the genotype on the metabolic pathways, e.g., knockout or insertion of genes [7].

On the other hand, kinetic models are valuable tools that can provide quantitative predictions for well studied systems. In spite of the difficulty in obtaining kinetic parameters, large-scale models are now available and it is expected their number, complexity and accuracy will increase in the coming years [8, 9]. Kinetic models allow us to determine the enzyme levels needed to accomplish optimal production of a

given metabolite [1, 10]. Moreover, kinetic models make possible the analysis of stability of the predicted states, an issue that is important in view of the fact that biological systems may exhibit not only monotonic stable states but also bistable switching threshold phenomena, oscillations and chaotic behavior [11]. In *E. coli* multistability and oscillations have been observed in strains designed for these purposes as well as for strains modified for different objectives [12-15]. Furthermore, in practice the precise modulation of enzyme levels is not attainable yet, therefore it is important to know the behavior of the system in the neighborhood of the desired values.

Due to the nonlinear kinetics of the biochemical reactions and their coupling through common metabolites, biological systems may be subject to drastic changes in their qualitative behavior when subjected to variation of the enzyme levels, e.g., loss of stability, switching to a different steady state, limit cycle oscillations. Bifurcation analysis allows the identification of critical points in the parameter space where these changes take place. Many contributions have been made to the analysis of complex dynamic phenomena in nonlinear chemical reactions systems. These mathematical tools have been used extensively in the analysis of biological systems [12, 16-20], however, small or moderate size models have been analyzed.

To the best of our knowledge, there have been no results on the construction of bifurcation diagrams for large-scale kinetic models of a metabolic system. In this work we constructed bifurcation diagrams for a large-scale kinetic model to analyze the sensitivity and the stability properties of a kinetic representation of the central carbon metabolism of *E. coli* at optimal enzyme levels, obtained through the solution of a nonlinear optimization problem. The bifurcation parameters considered are the maximum reaction rates sets of one, two and three enzymes for the optimal and suboptimal production of serine, as determined by [1].

## II. THE MODEL AND THE OPTIMAL ENZYME SETS

The model used in this work is an adaptation of the model of the central metabolism of *E. coli* presented in [8] and is shown in Fig. 1. It considers the glucose transport system, glycolysis, the pentose-phosphate pathway and simplifications of the biosynthetic and anaplerotic reactions. It comprises of 30 reactions and 17 primary metabolites. The concentrations of secondary metabolites or cofactors (i.e., ATP, ADP, AMP, NAD, NADH, NADP, and NADPH)

This work was supported in part by the Pennsylvania State University, Dean's Fund, and DOE 02-05ER25684.000. F. G. Vital-Lopez (e-mail: [fgv101@psu.edu](mailto:fgv101@psu.edu)), C. D. Maranas (e-mail: [costas@psu.edu](mailto:costas@psu.edu)) and A. Armaou (e-mail: [armaou@engr.psu.edu](mailto:armaou@engr.psu.edu)) are with The Pennsylvania State University, University Park, PA, 16802, USA.

\*Corresponding author: phone: 814 865 5316; fax: 814 965 7846.

and extracellular glucose are kept constant [8]. The model can be written as:

$$\frac{dC_i}{dt} = \sum_{j=1}^M S_{ij} \cdot r_j(r_j^{\max}, \mathbf{C}, \mathbf{K}), \quad \forall i = 1, \dots, N, \quad (1)$$

where  $C_i$  is the concentration of metabolite  $i$ ,  $S_{ij}$  is the stoichiometric coefficient of metabolite  $i$  in reaction  $j$ ,  $r_j$  and  $r_j^{\max}$  are the reaction rate and maximum reaction rate of reaction  $j$ ,  $\mathbf{C}$  is the concentration vector,  $\mathbf{K}$  is the vector of kinetic parameters,  $M$  is the number of enzymes, and  $N$  is the number of metabolites. The kinetic rate expressions can be expressed as a factor of the maximum reaction rates and a nonlinear function of the concentration of metabolites:

$$r_j = r_j^{\max} f_j(\mathbf{C}). \quad (2)$$

The maximum reaction rates are good candidates as parameters to be tuned in order to modify the behavior of the biological system since they can be related to the level of the corresponding enzymes; it is assumed that the maximum reaction rate is proportional to the enzyme level. Since currently the targeted modulation of all of the enzymes in a system is not feasible, in [1] a methodology was proposed to determine optimal enzyme sets and levels to enhance or suppress capabilities of cellular systems. The approach was illustrated by determining the optimal and suboptimal enzyme sets to enhance the production of serine, using the kinetic model mentioned above. The optimal sets of one, two and three enzymes that were identified and that will be used to construct the bifurcation diagrams are shown in Table I.

The methodology proposed in [1] determines enzyme level modulations that result in a total protein levels close to that of the original system. This requirement was included in view of the fact that large changes in protein levels may result in significant physiological changes not considered in the kinetic model [21]. Mathematically, this requirement was expressed by the following constraints:

$$\frac{1}{M} \sum_{j=1}^M \frac{r_j^{\max}}{r_j^{\max,0}} = 1, \quad \frac{r_{j_1}^{\max}}{r_{j_1}^{\max,0}} = \dots = \frac{r_{j_K}^{\max}}{r_{j_K}^{\max,0}}, \quad (3)$$

where  $r_j^{\max,0}$  is the maximum reaction rate at the reference state,  $j_1, \dots, j_K$  are the indices of non-modulated enzymes,  $K = M - L$ , and  $L$  is the number of modulated enzymes. These constraints were considered in the construction of the bifurcation diagrams in accordance with the results of [1]. They imply that if the level of an enzyme increases, the levels of the other enzymes should decrease maintaining the

TABLE I  
BIFURCATION PARAMETERS\*

One parameter	Two parameters	Three parameters
SerSynth (0.0257)	SerSynth, PTS (7830)	
PGM (89.05)	SerSynth, PK (0.0611)	
ENO (330.4)	SerSynth, PepCxlase (0.107)	SerSynth, PFK (1841), and PepCxlase
DAHPS (0.108)	SerSynth, PDH (6.06)	
Synth1(0.0195)	SerSynth, Synth2(0.0736)	

\*The parameters are the maximum reaction rates of the corresponding enzymes. The number in parenthesis correspond to their reference values. See caption of Fig. 1 for nomenclature.

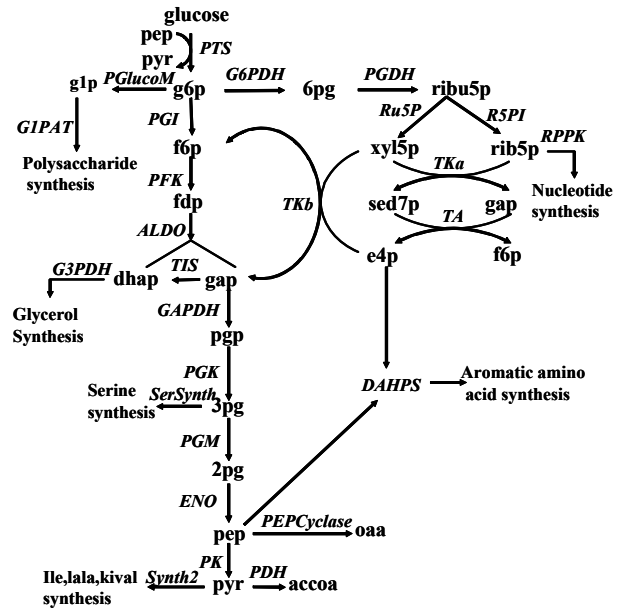


Fig. 1. Central carbon metabolism of *E. coli*. **Enzymes:** aldolase (ALDO), DAHP synthase (DAHPS), enolase (ENO), glucose-1-phosphate adenylyltransferase (GIPAT), glycerol-3-phosphate dehydrogenase (G3PDH), glucose-6-phosphate dehydrogenase (G6PDH), glyceraldehyde-3-phosphate dehydrogenase (GAPDH), methionine synthesis (MetSynth), mureine synthesis (MurSynth), phosphofructokinase (PFK), 6-phosphogluconate dehydrogenase (PGDH), glucose-6-phosphate isomerase (PGI), phosphoglycerate kinase (PGK), phospho-glycerate mutase (PGM), pyruvate dehydrogenase (PDH), PEP carboxylase (PEPcylase), phosphoglucomutase (PGLuCoM), pyruvate kinase (PK), phospho-transferase system (PTS), ribose-phosphate isomerase (R5PI), ribose-phosphate pyrophosphokinase (RPPK), ribulose-phosphate epi-merase (Ru5P), Serine synthesis (SerSynth), synthesis1 (Synth1), synthesis2 (Synth2), transaldolase (TA), triosephosphate iso-merase (TIS), transketolase A (TKa), transketolase B (TKb), tryptophan synthesis (TrpSynth). **Metabolites:** 1,3-diphosphoglycerate (p3g), 2-phospho-glycerate (2PG), 3-phospho-glycerate (3PG), 6-phosphogluconate (6PG), acetyl-coenzyme A (accoa), dihydroxyacetonephosphate (dhap), erythrose-4-phosphate (e4p), fructose-6-phosphate (f6p), fructose-1,6-bisphosphate (fdp), glucose-1-phosphate (g1p), glucose-6-phosphate (g6p), glyceraldehyde-3-phosphate (gap), glucose (glc), oxaloacetate (oaa), phosphoenolpyruvate (pep), pyruvate (pyr), ribose-5-phosphate (rib5P), ribulose-5-phosphate (ribu5p), sedoheptulose-7-phosphate (sed7p), xylulose-5-phosphate (xyl5p).

same proportion as in the reference state, such that the total level of enzymes remains constant.

### III. BIFURCATION ANALYZIS

The bifurcation diagrams were constructed using a pseudo arc-length continuation technique with a predictor-solver scheme [22, 23]. The procedure consists of finding a point in the branch solution and using this information to calculate a solution on the branch close to the previous solution as the parameters vary. To calculate the new solution, the predictor provides an adequate initial guess that is used in the corrector step to obtain the new solution. For the current work, the secant method was used as the predictor:

$$C_i^{\text{pred}} = C_i^0 + \frac{ds}{s_0 - s_{-1}} (C_i^0 - C_i^{-1}) \quad \forall i \in N, \quad (4a)$$

$$l_k^{\text{pred}} = l_k^0 + \frac{ds}{s_0 - s_{-1}} (l_k^0 - l_k^{-1}), \quad (4b)$$

$$s_{\text{pred}} = s_0 + ds, \quad (4c)$$

where  $C_i^{\text{pred}}$  is the predicted concentration of metabolite  $i$ ,  $C_i^0$  and  $C_i^{-1}$  are concentrations calculated in the two previous

iterations. Similarly,  $l_k^{pred}$  is the predicted bifurcation parameter and  $l_k^0$  and  $l_k^{-1}$  are the last two calculated parameters;  $s$  is arclength of the solution branch and  $ds$  the length step.

In the corrector step, for the case of one parameter, the system (1) is augmented with the equation:

$$ds - \sum_{i=1}^N \frac{|C_i - C_i^0|}{C_i^{ref}} - \sum_{k=1}^P \frac{|l_k - l_k^0|}{l_k^{ref}} = 0, \quad (5)$$

where  $C_i^{ref}$  and  $l_k^{ref}$  are the concentration of metabolite  $i$  and the value of parameter  $k$  at the reference state respectively;  $P$  is the number of bifurcation parameters. The system is then solved using  $C_i^{pred}$  and  $l_k^{pred}$  as initial guess. Equation (5) confers stability to the continuation method close to the points where the original continuation method does not converge to a solution (i.e., the Jacobian of the linearized model is singular) and allows passing these points. The bifurcation points were identified as the points where one or a pair of eigenvalues of the Jacobian of the linearized system crosses the imaginary axis. The augmented system was solved with the MatLab subroutine `fsolve`.

In order to construct the bifurcation maps for the case of two parameters an additional equation is needed:

$$\min_{i=1, \dots, N} |\operatorname{Re}(eig_i)| = 0, \quad (6)$$

where  $eig_i$  are the eigenvalues of Jacobian of the linearized system evaluated at the solution. This equation allows the calculation of the second parameter at the point where the system experiences a bifurcation, i.e., one or two eigenvalues of the Jacobian of the linearized system have zero real part.

In the case of three parameters, the bifurcation map was constructed in a similar way as in the case of two parameters. Specifically, the parameter  $r_{PepCysylase}^{max}$  was held constant and bifurcation maps on  $r_{SerSynth}^{max}$  and  $r_{PFK}^{max}$  were constructed for several values of the constant parameter.

In order to satisfy constraint (3), in all cases the maximum reaction rates that were not used as bifurcation parameters, were adjusted according to:

$$r_{j^k}^{max} = r_{j^k}^{max,0} \left( N - \sum_{i=1}^n \frac{l_i}{l_i^{ref}} \right) \frac{1}{N - n}, \quad (7)$$

where  $n$  is the number of bifurcation parameters.

#### IV. RESULTS

In this section, the stability and sensitivity analyses of the central carbon metabolism of *E. coli* are presented. In the first subsection we describe the bifurcation diagrams for one parameter, as well as a limit cycle that the system exhibits. The cases for two and three parameter variations are discussed in the sequel subsections.

##### A. One parameter

We initially employed  $r_{SerSynth}^{max}$  as our bifurcation parameter. The system undergoes two bifurcations when this parameter is varied, shown in Fig. 2(a). Starting at the reference

state,  $r_{SerSynth}^{max,0}$ , the system goes through a Hopf bifurcation and subsequently it goes through a limit point when  $r_{SerSynth}^{max}$  becomes  $9.8 r_{SerSynth}^{max,0}$  and  $13.6 r_{SerSynth}^{max,0}$ , respectively. The system has three equilibrium points for  $r_{SerSynth}^{max} = 13.6 r_{SerSynth}^{max,0}$  (for all cases investigated, there is a stable solution branch at very low concentrations which is not presented in the figures). After the limit point only the solution branch at very low concentrations exists. The upper branch is stable for  $r_{SerSynth}^{max} < 9.8 r_{SerSynth}^{max,0}$ , and it becomes unstable for  $r_{SerSynth}^{max} > 9.8 r_{SerSynth}^{max,0}$  (with branch instability we imply that the system is unstable in the neighborhood of the steady state for the specific process parameters and that the trajectories converge to the steady state at low concentrations). The lower branch is unstable for all the parameter values where it exists. At the Hopf bifurcation a limit cycle appears, which is stable as implied through simulations, shown in Fig. 3. This figure depicts the trajectories of the system on the plane  $C_{3pg}-C_{g6p}$  for two different initial states, one inside the limit cycle and the other outside. It is observed that in both cases the trajectories converge to the limit cycle. For  $r_{SerSynth}^{max} = 0.252$  the limit cycle is stable with a mean value for the synthesis rate of serine equal to  $0.028 \text{ mM}\cdot\text{s}^{-1}$ , while the amplitude and the period are  $0.044 \text{ mM}\cdot\text{s}^{-1}$  and  $397.5 \text{ s}$  respectively.

We also observe in Fig. 2(a) that the synthesis rate of serine is, as expected, highly sensitive to changes in  $r_{SerSynth}^{max}$ . Moreover, we observe that the constraint on the total change allowed in the concentration for the optimization prevents the synthesis rate of serine from reaching its maximum value when such constraint is disregarded. In such case, the optimal value for the synthesis rate of serine corresponds to  $r_{SerSynth}^{max} = 0.13$  and the concentration deviation from the reference state is 42%.

Next, we present the result of analyzing the systems to changes on  $r_{PGM}^{max}$ . The system has three steady states for  $8 \times 10^{-4} r_{PGM}^{max,0} \leq r_{PGM}^{max} \leq 30 r_{PGM}^{max,0}$ , shown in Fig. 2(b). The lower bound corresponds to a limit point; beyond this point the system has only one solution branch at very low concentrations. The upper bound is due to constraint (3). In the diagram, the upper branch belongs to the stable steady states while the lower branch to the unstable ones. Even though the limit point occurs at small  $r_{PGM}^{max}$ , there is not a feasible point for  $r_{PGM}^{max} = 0$ . The bifurcation diagram for  $r_{ENO}^{max}$  is qualitatively similar to the diagram for  $r_{PGM}^{max}$ , and for reasons of brevity it is omitted; the limit point then occurs at  $r_{ENO}^{max} = 2.9 \times 10^{-4} r_{ENO}^{max,0}$ . In both cases, the synthesis rate of serine has low sensitivity with respect to changes in these parameters, even though they were identified as optimal candidates to increase the production of serine.

The case of  $r_{Synth1}^{max}$  is presented in Fig. 2(c). The system undergoes a Hopf bifurcation at  $r_{Synth1}^{max} = 10.4 r_{Synth1}^{max,0}$  and goes through a limit point at  $r_{Synth1}^{max} = 14 r_{Synth1}^{max,0}$ , and it has three equilibrium points for  $r_{Synth1}^{max} = 14 r_{Synth1}^{max,0}$ , (one of them is the solution branch at very low concentrations, not presented in

the figure). The upper branch is stable before the Hopf bifurcation, at which point it becomes unstable. The lower branch is unstable for all values of  $r_{Synth1}^{max}$ . In Fig. 2(c) we can also observe that the synthesis rate of serine is sensitive to changes on  $r_{Synth1}^{max}$ , and that the lower bound ( $r_{Synth1}^{max}=0$ ) prevents the synthesis rate of serine from further increasing. For  $r_{DAPHS}^{max}$  the bifurcation diagram has only one branch and it is not presented here. In these two cases the system is

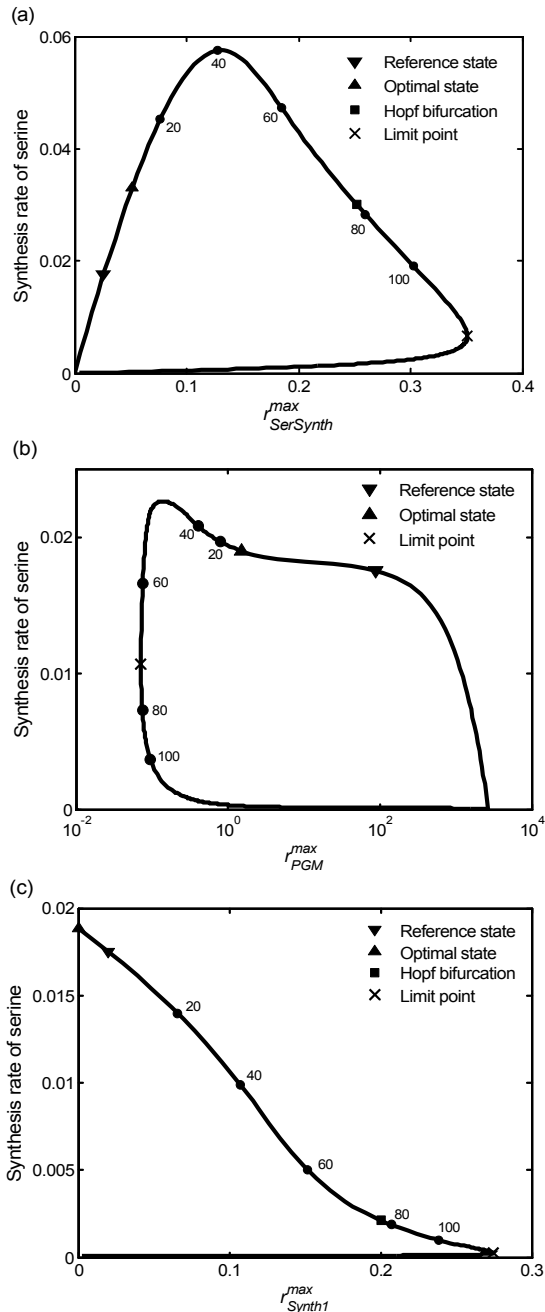


Fig. 2. Bifurcation diagrams for one parameter presenting the synthesis rate of serine as a function of: (a) for maximum reaction rate for the serine synthesis pathway; (b) maximum reaction rate of PGM; (c) maximum reaction rate of Synth1. The solid lines denote the steady state of the system. The round marks, tagged with small numbers, indicate the percentage of deviation of the concentrations with respect to the reference state.  $\nabla$ ,  $\blacktriangle$ ,  $\blacksquare$ , and  $\times$  represent the reference state, the optimal state, the Hopf bifurcation, and the limit point, respectively.

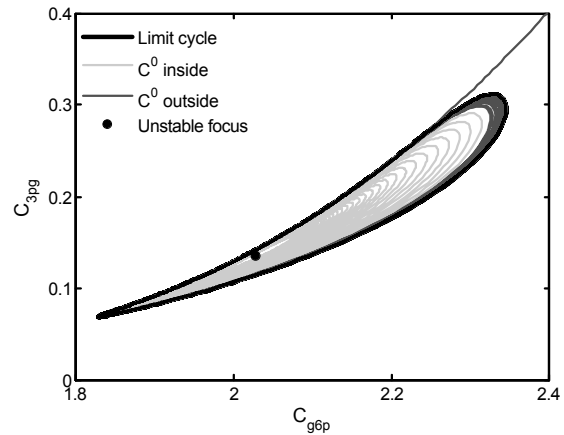


Fig. 3. Phase plane of a limit cycle when  $r_{SerSynth}^{max} = 0.252$ . The diagram shows the trajectories of the concentrations of glucose-6-phosphate ( $C_{66p}$ ) and 3-phosphoglycerate ( $C_{3pg}$ ). The synthesis rate of serine is an explicit function of 3-phosphoglycerate. The gray lines are trajectories with initial states in and out of the limit cycle. The black line corresponds to the limit cycle;  $\bullet$  represents the unstable focus.

stable under any perturbation of the parameters since in the case of  $r_{Synth1}^{max}$  the flux is set to zero, and in the case of  $r_{DAPHS}^{max}$  no bifurcations are present.

### B. Two parameters

In [1] it was found that the synthesis rate of serine was sensitive to  $r_{SerSynth}^{max}$ ; as a result, the pairs considered in this paper comprise of  $r_{SerSynth}^{max}$  and another parameter. The bifurcation maps constructed track the loci of the Hopf bifurcation and the limit point on the plane formed by the respective pair of parameters. For the identified optimal pair  $r_{PTS}^{max}$  and  $r_{SerSynth}^{max}$ , the reference state and the optimum state lie close to the Hopf bifurcation, requiring a 68% and 100% change on  $r_{PTS}^{max}$  with respect to  $r_{PTS}^{max,0}$  respectively; shown in Fig. 4(a). This is an important result since the imprecision associated with modulating enzyme levels can drive the system to become unstable. Furthermore, the Hopf bifurcation and the limit point lie very close. In fact for a wide range of parameter values they practically overlap. However, the concentrations differ considerably between the Hopf bifurcation and the limit point. This is because close to the limit point the concentrations are very sensitive to the parameters values.

For the pair  $r_{SerSynth}^{max} - r_{PK}^{max}$ , the loci of both the Hopf bifurcation and the limit point are practically linear with respect to this pair of parameters, shown in Fig. 4(b). A reduction in  $r_{PK}^{max}$  results in increasing the system robustness to perturbations (i.e., the possibility of increasing  $r_{SerSynth}^{max}$  further before the system becomes unstable). The bifurcation map for the pair  $r_{SerSynth}^{max} - r_{PepCylase}^{max}$  is qualitatively similar to the previous one and is omitted for brevity. For the case of  $r_{SerSynth}^{max} - r_{PDH}^{max}$  the bifurcation map, shown in Fig. 4(c), is qualitatively similar to  $r_{PTS}^{max}$ , but the distance between the Hopf bifurcation and the limit point is considerably larger. In this case the optimal state is located far from the bifurcation implying that the modulation not only increases the serine

production but also confers bigger stability margins to the system. The  $r_{SerSynth}^{max} - r_{Synth2}^{max}$  diagram is also qualitatively similar to  $r_{PTS}^{max}$  and is omitted for brevity. For  $r_{Synth2}^{max} < 4r_{Synth2}^{max,0}$  the distance between the Hopf bifurcation and the limit point is considerable, but for  $r_{Synth2}^{max} > 4r_{Synth2}^{max,0}$  they practically overlap, as in the  $r_{PTS}^{max}$  case. Contrary to the  $r_{PTS}^{max}$  case, the optimum state is far away from any bifurcation points, which implies that the system is then robust to uncertainty in these parameters.

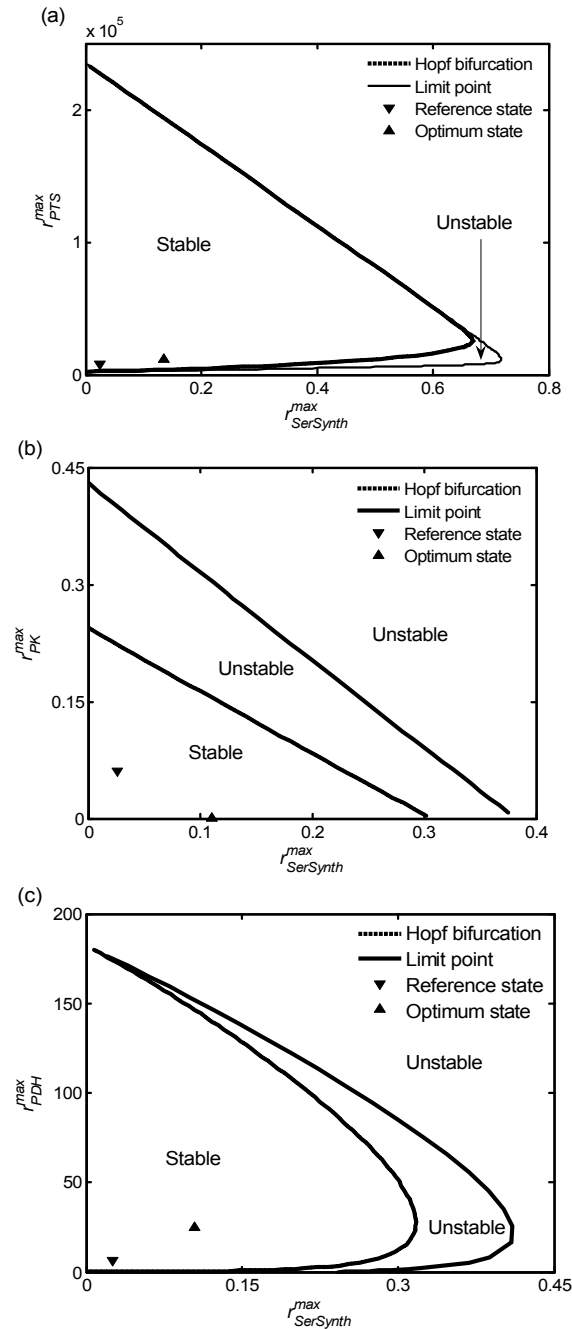


Fig. 4. Bifurcation maps presenting the qualitative behavior of the system in the parameter space for: (a)  $r_{SerSynth}^{max}$  and  $r_{PTS}^{max}$ ; (b)  $r_{SerSynth}^{max}$  and  $r_{PK}^{max}$ ; (c)  $r_{SerSynth}^{max}$  and  $r_{PDH}^{max}$ . The dashed line, the solid line,  $\nabla$ , and  $\blacktriangle$  represent the Hopf bifurcation, the limit point respectively, the reference state, and the optimal state, respectively.

### C. Three parameters

For the case of three parameters only the optimal triplet was investigated. In Fig. 5(a) we present a bifurcation map on the plane  $r_{SerSynth}^{max} - r_{PFK}^{max}$  for  $r_{PepCyclase}^{max} = 0.0001$ , corresponding to its optimal value. Notice that the reference state (for which  $r_{PepCyclase}^{max} = 0.11$ ) and the optimal state lie close to the Hopf bifurcation. Taking into account the difficulty to modulate the enzyme levels precisely, this implies that a relatively large deviation on the enzyme levels from their desired value may provoke the system to become unstable. Furthermore for  $10.1r_{PFK}^{max,0} < r_{PFK}^{max} < 19.1r_{PFK}^{max,0}$ , the system undergoes two Hopf bifurcations when  $r_{SerSynth}^{max}$  is varied. As  $r_{SerSynth}^{max}$  increases the system goes through a Hopf bifurcation and a limit cycle, which is stable for a small set of parameter values, appears. Subsequently, the limit cycle becomes unstable and disappears for  $r_{PFK}^{max} < 13r_{PFK}^{max,0}$ . Close to the second Hopf bifurcation a limit cycle appears again and becomes stable only for a small set of parameter values close to the bifurcation. After the second Hopf bifurcation the system becomes a stable node. Further increase of  $r_{SerSynth}^{max}$  leads the system through a limit point. Beyond the limit point, only the steady state at very low concentrations remains.

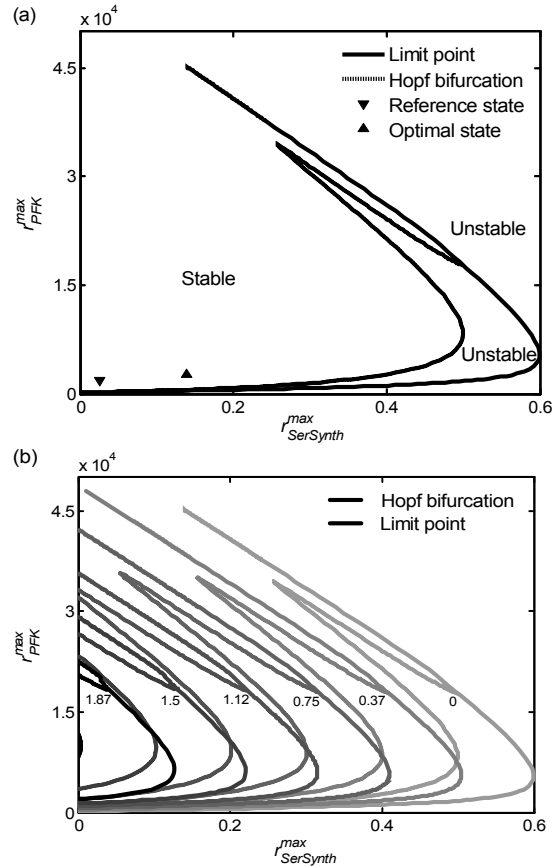


Fig. 5. Bifurcation map presenting the behavior of the system on the parameter space for  $r_{SerSynth}^{max}$ ,  $r_{PFK}^{max}$  and  $r_{PepCyclase}^{max}$ . (a) A single contour of the bifurcation map on the  $r_{SerSynth}^{max}$  vs.  $r_{PFK}^{max}$  for  $r_{PepCyclase}^{max} = r_{PepCyclase}^{max,0}$ . (b) Contours for constant values of  $r_{PepCyclase}^{max}$  as indicated by the numbers inside the figure. The dashed line, the solid line,  $\nabla$ , and  $\blacktriangle$  represent the Hopf bifurcation, the limit point respectively, the reference state, and the optimal state, respectively.

The effect of  $r_{PepCxyIase}^{\max}$  on the behavior of the system is presented in Fig. 5(b). It shows contours of the loci of the Hopf bifurcation and the limit point on the plane  $r_{SerSynth}^{\max} - r_{PFK}^{\max}$  for constant values of  $r_{PepCxyIase}^{\max}$  (indicated by the numbers inside the figure). It can be observed that as  $r_{PepCxyIase}^{\max}$  increases the system undergoes the Hopf bifurcation and goes through the limit point for smaller values of  $r_{SerSynth}^{\max}$ . This can be explained by the fact that as  $r_{PepCxyIase}^{\max}$  increases there is less resources available for construction of the rest of enzymes due to constraint (3). For  $r_{PepCxyIase}^{\max} > 1.87$  the system is unstable regardless the values of  $r_{SerSynth}^{\max} - r_{PFK}^{\max}$ .

## V. DISCUSSION

The stability properties of the kinetic model describing the metabolism of *E. coli* were assessed by constructing bifurcation diagrams for the optimal parameters for the production of serine. The bifurcation diagrams show that the central carbon metabolism of *E. coli* can exhibit oscillatory (and in general highly nonlinear) behavior for certain values of the parameters. The system undergoes a Hopf bifurcation and goes through a limit point when the level of specific parameters is varied, and the system exhibits sustained oscillations close to the Hopf bifurcation. Further variation of the parameters leads to the disappearance of the limit cycle and the system becomes unstable. However, the reference state and the analyzed optimal states are usually distant from the bifurcation point (requiring more than 68% change in the parameter values), suggesting that the optimal states are attainable and the system is robust to perturbations on enzyme levels. Finally, although we do not have experimental evidence, from our analysis we observe that the system may undergo sustained oscillations in a small range of parameter values.

## VI. ACKNOWLEDGMENT

We are grateful to Professors Reuss and Schmid for providing us with the detailed kinetic model.

## VII. REFERENCE

- [1] E. V. Nikolaev, P. Pharkya, C.D. Maranas, and A. Armaou, "Optimal selection of enzyme levels using large-scale kinetic models.," presented at *Proceedings of 16<sup>th</sup> I.F.A.C. World Congress*, to appear, Prague, Czech Republic, 2005.
- [2] A. Seressiotis and J. E. Bailey, "MPS: an artificially intelligent software system for the analysis and synthesis of metabolic pathways," *Biotechnol Bioeng*, vol. 31, pp. 587-602, 1988.
- [3] G. Stephanopoulos and T. W. Simpson, "Flux amplification in complex metabolic networks," *Chemical Engineering Science*, vol. 52, pp. 2607-2627, 1997.
- [4] C. H. Schilling, S. Schuster, B. O. Palsson, and R. Heinrich, "Metabolic pathway analysis: basic concepts and scientific applications in the post-genomic era," *Biotechnol Prog*, vol. 15, pp. 296-303, 1999.
- [5] S. Schuster, T. Dandekar, and D. A. Fell, "Detection of elementary flux modes in biochemical networks: a promising tool for pathway analysis and metabolic engineering," *Trends Biotechnol*, vol. 17, pp. 53-60, 1999.
- [6] N. D. Price, J. L. Reed, J. A. Papin, I. Famili, and B. O. Palsson, "Analysis of metabolic capabilities using singular value decomposition of extreme pathway matrices," *Biophys J*, vol. 84, pp. 794-804, 2003.
- [7] P. Pharkya, A. P. Burgard, and C. D. Maranas, "Exploring the overproduction of amino acids using the bilevel optimization framework OptKnock," *Biotechnol Bioeng*, vol. 84, pp. 887-99, 2003.
- [8] C. Chassagnole, N. Noisommit-Rizzi, J.W. Schmid, K. Mauch, and M. Reuss, "Dynamic modeling of the central carbon metabolism of *Escherichia coli*," *Biotechnol Bioeng*, vol. 79, pp. 53-73, 2002.
- [9] M. Tomita, K. Hashimoto, K. Takahashi, T. Shimizu, Y. Matsuzaki, F. Miyoshi, K. Saito, S. Tanida, K. Yugi, J. C. Venter, and C. A. Hutchison, "E-CELL: Software Environment for Whole Cell Simulation," *Genome Inform Ser Workshop Genome Inform*, vol. 8, pp. 147-155, 1997.
- [10] D. Visser, J. W. Schmid, K. Mauch, M. Reuss, and J. J. Heijnen, "Optimal re-design of primary metabolism in *Escherichia coli* using linlog kinetics," *Metab Eng*, vol. 6, pp. 378-90, 2004.
- [11] D. Lloyd, M. A. Aon, and S. Cortassa, "Why homeodynamics, not homeostasis?," *ScientificWorldJournal*, vol. 1, pp. 133-45, 2001.
- [12] E. Fung, W. W. Wong, J. K. Suen, T. Bulter, S. G. Lee, and J. C. Liao, "A synthetic gene-metabolic oscillator," *Nature*, vol. 435, pp. 118-22, 2005.
- [13] D. C. Andersen, J. Swartz, T. Ryll, N. Lin, and B. Snedecor, "Metabolic oscillations in an E-coli fermentation," *Biotechnology and Bioengineering*, vol. 75, pp. 212-218, 2001.
- [14] J. Weber, A. Kayser, and U. Rinas, "Metabolic flux analysis of *Escherichia coli* in glucose-limited continuous culture. II. Dynamic response to famine and feast, activation of the methylglyoxal pathway and oscillatory behaviour," *Microbiology-Sgm*, vol. 151, pp. 707-716, 2005.
- [15] E. M. Ozbudak, M. Thattai, H. N. Lim, B. I. Shraiman, and A. van Oudenaarden, "Multistability in the lactose utilization network of *Escherichia coli*," *Nature*, vol. 427, pp. 737-740, 2004.
- [16] D. D. J. E. B. Bruns, D. Luss, "Steady state multiplicity and stability of enzymatic reactions," *Biotechnol Bioeng*, vol. 15, pp. 1131-1145, 1973.
- [17] V. Hatzimanikatis and J. E. Bailey, "Studies on glycolysis .1. Multiple steady states in bacterial glycolysis," *Chemical Engineering Science*, vol. 52, pp. 2579-2588, 1997.
- [18] J. J. Tyson, K. Chen, and B. Novak, "Network dynamics and cell physiology," *Nat Rev Mol Cell Biol*, vol. 2, pp. 908-16, 2001.
- [19] A. Arkin, J. Ross, and H. H. McAdams, "Stochastic kinetic analysis of developmental pathway bifurcation in phage lambda-infected *Escherichia coli* cells," *Genetics*, vol. 149, pp. 1633-48, 1998.
- [20] W. M. Haddad and V. Chellaboina, "Stability and dissipativity theory for nonnegative dynamical systems: a unified analysis framework for biological and physiological systems," *Nonlinear Analysis-Real World Applications*, vol. 6, pp. 35-65, 2005.
- [21] K. Mauch, S. Buziol, J. Schmid, and M. Reuss, "Computer-aided design of metabolic networks. In Rawlings, J., Ogunnaike, T., Eaton, J. (Eds.)," *AIChE Symposium Series*, vol. 98, pp. 82-91, 2002.
- [22] G. M. Shroff, and H.B. Keller, "Stabilization of unstable procedures: The recursive projection method.," *SIAM Journal on Numerical Analysis*, vol. 30, pp. 1099-1120, 1993.
- [23] R. Seydel, and Hlavacek, V., "Role of continuation in engineering analysis," *Chemical Engineering Science*, vol. 42, pp. 1281-1295, 1987.